J. Biochem. 124, 528-533 (1998)

A Unique Loop Contributing to the Structure of the ATP-Binding Cleft of Skeletal Muscle Myosin Communicates with the Actin-Binding Site

Shinsaku Maruta[1] and Kazuaki Homma

Department of Bioengineering, Faculty of Engineering, Soka University, 1-236 Tangi-machi, Hachioji, Tokyo 192-8577

Received for publication, March 6, 1998

Actin binding to skeletal muscle myosin subfragment-1 (S1) increases the dissociation rate of reaction products from the myosin ATPase site; conversely, ATP binding facilitates dissociation of complexed acto-S1. However, details of the molecular mechanism by which the ATP- and actin-binding sites communicate with each other is still obscure. We present evidence that the effect of actin is mediated by a conformational change in the loop containing amino acids from 677 to 689 [loop M (677-689)], a segment of the 20-kDa tryptic fragment that contributes to the structure of the ATP-binding cleft. Initially, a fluorescent ADP analogue, methylanthranyloyl-8-azido-ADP (Mant-8-N_3-ADP), was covalently crosslinked to loop M (Mant-S1), perhaps at Lys 681. Actin-activated Mg^{2+}-ATP hydrolysis by Mant-S1 was accelerated approximately 6 times over that by unmodified S1, suggesting that the ATPase site is not blocked by the ADP analogue crosslinked in the loop M (677-689). Nevertheless, analysis of Mant-group fluorescence polarization and acrylamide-induced quenching showed the crosslinked probe to be entrapped within the ATP-binding cleft at a location where Mant-group rotational mobility was hindered, and where it was relatively inaccessible to the solvent. Exposing Mant-S1 to Mg^{2+}-ATP and/or actin elicited similar decreases in fluorescence polarization, indicating increased rotational mobility of the Mant-group and movement of crosslinked Mant-8-N_3-ADP to a less hindered position. Stern-Volmer quench curves showed that Mant-8-N_3-ADP was translocated to a site where it was more accessible to dissolved quencher, perhaps outside the ATP-binding cleft. Since actin does not bind to the ATPase site, actin-induced translocation of Mant-8-N_3-ADP crosslinked to loop M (677-689) probably results from a conformational change in loop M (677-689). These results suggest that loop M acts as a signal transducer mediating communication between the ATP- and actin-binding sites.

Key words: ATP analogue, ATP binding site, fluorescent polarization, myosin, signal transduction.

Muscle contraction is driven by the hydrolysis of ATP by myosin, but our understanding of the process through which energy released by the hydrolysis is converted into mechanical work is incomplete (*1, 2*). It is known that once Mg^{2+}-ATP binds to the ATPase site, hydrolysis proceeds rapidly, and because dissociation of the reaction products is comparatively slow, an equilibrium is readily established between myosin-ATP and myosin**-ADP-P_i (*3*). The reaction is pulled in the direction of ATP hydrolysis by the binding of actin, which greatly increases the dissociation rates of ADP and P_i. However, actin does not bind to the ATPase site, and the specific molecular mechanism by which actin augments dissociation of ADP and P_i is still unknown.

Recent crystallographic studies of motor proteins showed that the structures of the motor domains of myosin (*4*) and kinesin (*5*) are highly conserved. Thus, these motor proteins may share a common mechanism for generating energy for motility from ATP hydrolysis. Nevertheless, myosin has several unique loops in the region of the ATP-binding cleft which have not been observed in kinesin (*4*). The precise function of the loops is as yet unknown, but they may have roles in determining the characteristic properties of myosin: *e.g.*, mediating the interaction of the ATP- and actin-binding sites.

Loop M (677-689), which is part of the 20-kDa tryptic fragment of skeletal S1, is unique to myosin and contributes to the structure of the ATP-binding cleft; a key feature of the loop is Lys 681, which protrudes into ATP-binding site (Fig. 1). Composed mainly of α-helix, the 20-kDa fragment forms the backbone of the myosin head and extends from the actin-binding site to the regulatory region, *via* the ATP binding site, and to the hinge area of the reactive cystein region (Fig. 1A). This arrangement means

[1] To whom correspondence should be addressed. Phone: +81-426-91-9443, Fax: +81-426-91-9312, E-mail: shinsaku@t.soka.ac.jp

Abbreviations: S1, myosin subfragment-1; Mant-8-N_3-ADP, 3′-*O*-(*N*-methylanthraniloyl)-8-azido-ADP; Mant-S1, Mant-8-N_3-ADP covalently crosslinked to S1; NANDP, 2-[(4-azido-2-nitrophenyl)-amino]ethyl diphosphate; Bz_2-ADP, 3′-*O*-benzoylbenzoic-ADP; Bz_2-εADP, 3′-*O*-benzoylbenzoic-1,N^6-etheno-ADP; BeF_x, fluoroberyllate; SDS-PAGE, sodium dodecyl sulfate polyacryl amide gel electrophoresis.

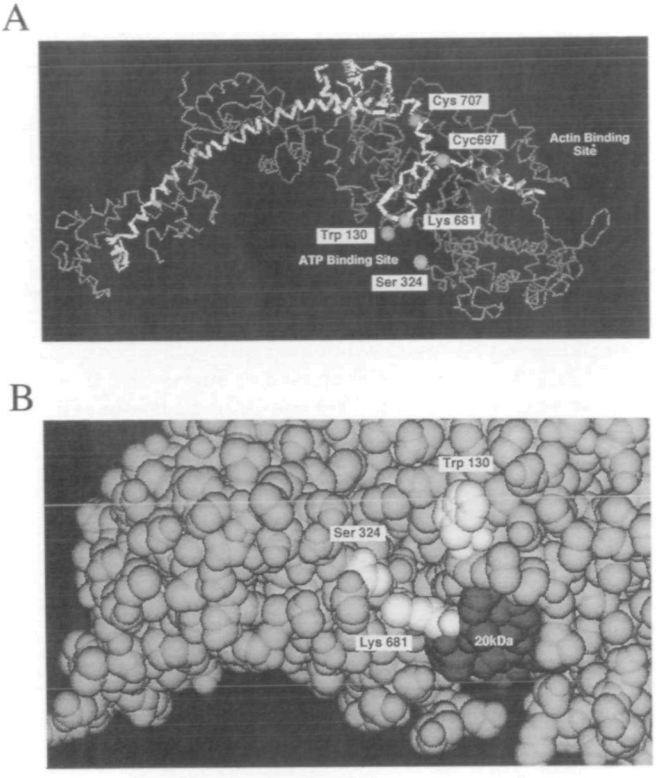

Fig. 1. **A: A ribbon representation of the 20-kDa tryptic fragment within the myosin S1 tertiary structure.** Reactive cystein residues and ATP analogue crosslinked amino acids are indicated by their respective space-filling α-carbons. **B: A space-filling representation of the ATP-binding cleft of myosin S1.** Note that the side chain of Lys 681 in the 20-kDa fragment protrudes into the ATP-binding cleft. These figures were prepared with the molecular graphic program MacImdad Version 5 (Molecular Applications Group) using the coordinate data (pdb. 2MYS) published by Rayment *et al.* in the protein data bank data base.

that the 20-kDa fragment and loop M (677-689) may provide the link through which ATPase activity is modulated by actin. For this reason, we focused on loop M (677-689) in trying to better understand the molecular mechanism underlying the interaction of the ATP- and actin-binding sites.

We previously demonstrated that the fluorescently labeled photoreactive ATP analogue, Mant-8-N_3-ATP, was specifically crosslinked to loop M by UV irradiation (*6*). In the present study, we covalently crosslinked the ADP analogue, Mant-8-N_3-ADP, to loop M (677-689) in order to monitor actin-induced conformational changes in the loop. Analysis of actin- and ATP-induced changes in fluorescence polarization and quenching confirmed that actin binding induces conformational changes at loop M (677-689) resulting in displacement of Mant-8-N_3-ADP from the ATP-binding cleft.

MATERIALS AND METHODS

Protein Preparations—Skeletal muscle myosin was prepared from chicken breast muscle by the method of Perry (*7*). The isolated myosin was then digested with α-chymotrypsin to obtain subfragment-1 (S1) as described by Weeds and Taylor (*8*). F-actin was purified from chicken skeletal muscle as described by Pardee and Spudich (*9*).

Chemicals—Mant-8-N_3-ATP was prepared from 8-N_3-ATP (Sigma) as described by Maruta *et al.* (*6*). Beryllium sulfate ($BeSO_4$) and sodium fluoride (NaF) were from Wako Pure Chemical (Tokyo).

Fluorescent Labeling of S1—Mant-8-N_3-ATP was hydrolyzed to Mant-8-N_3-ADP by incubation with S1. After complete hydrolysis, 1 mM $BeSO_4$ and 5 mM NaF were added to trap Mant-8-N_3-ADP at the active site. After incubation for 1 h at 25°C, untrapped analogue and BeFn were removed by centrifugal gel filtration on a Sephadex G-50 column (*10*) equilibrated in 120 mM NaCl and 50 mM Tris-HCl (pH 8.0). The solution containing the isolated ternary complex was then placed on ice and irradiated for 3 min with 366 nm UV light (UVL-56 16W, Ultraviolet Products).

Removal of Noncovalently Bound Mant-8-N_3-ADP and BeFn—Following UV irradiation, noncovalently bound analogue remaining in the ATPase site of S1 was removed by adding excess Mg^{2+}-ATP and actin according to Luo *et al.* (*11*). F-actin (2 ml, 100 μM) was pelleted by centrifugation at 350,000 $\times$ *g* for 20 min at 4°C; the supernatant was discarded, and the F-actin pellet was resuspended in 2 ml of the irradiated S1 solution. The 2 mM $MgCl_2$ and 2 mM ATP (pH 7.0) were added, and the solution was incubated at room temperature for 20 min to release trapped BeFn and the unincorporated Mant-8-N_3-ADP. To dissociate the actin, the ATP concentration was then increased to 4 mM, and the ionic strength was increased to 200 mM by addition of KCl at 4°C. The solution was then immediately centrifuged at 350,000 $\times$ *g* for 20 min at 4°C. EDTA (final concentration 20 mM) was added to the supernatant, which was then applied to Sephadex G-50 centrifugal column to remove Mg^{2+}, ATP, BeFn, and the released unincorporated ATP analogue. The resulting solution containing photolabeled S1 and unmodified S1 is hereafter referred to as the purified Mant-S1. After removing the free and noncovalently bound Mant-8-N_3-ADP, the amount of fluorescent probe covalently crosslinked to the ATPase site was estimated by measuring the fluorescence intensity of the remaining photolabeled product in a solution of 5 M guanidine-HCl and 20 mM Tris-HCl (pH 7.5).

SDS-PAGE—Electrophoresis was performed in 7.5-20% polyacrylamide gradient slab gels in the presence of 0.1% SDS at a constant voltage (200 V) in the discontinuous buffer system of Laemmli (*12*).

ATPase Assay—ATPase activity was measured in the presence of 2 mM ATP at 25°C. The reaction was stopped by addition of 10% trichloroacetic acid, and the released P_i was measured by the method of Youngburg and Youngburg (*13*).

Fluorescence Measurements—Fluorescence measurements were made at 25°C with an RF-5000 Spectrofluorometer (Shimadzu). In RF-5000, monochromatic light passes through an excitation filter (360 nm) and a moving polarizer and excites fluorescent molecules in the sample. The polarized light in the sample is emitted at right angles to the incident light and passes through an emission filter (445 nm) and a vertical fixed polarizer. The emitted light is measured in both horizontal (I_h) and vertical (I_v) planes, and polarization (P) is calculated from the equation $P = (I_v - I_h)/(I_v + I_h)$.

Calculation of the Stern-Volmer Quench Constant

(K_{sv})—Acrylamide quenching of Mant-8-N_3-ADP fluorescence was analyzed according to Stern and Volmer (*14, 15*). The Stern-Volmer quench constant was calculated from the equation: $F_0/F = 1 + K_{sv}[Q]$, where F_0 and F are fluorescence intensities in the absence and presence of quencher (acrylamide), respectively, K_{sv} is the Stern-Volmer quench constant, and [Q] is the concentration of acrylamide.

RESULTS

Specific Labeling of Loop M with Mant-8-N_3-ADP—To reduce nonspecific binding, Mant-8-N_3-ADP was trapped within the ATPase site by beryllium fluoride (BeFn) prior to UV photoirradiation. Maximal entrapment of Mant-8-N_3-ADP was achieved in the presence of a 2-fold molar excess of Mant-8-N_3-ADP (0.75 mol Mant-8-N_3-ADP/mol ATPase; Table I). Subsequent UV irradiation caused covalent linkage of Mant-8-N_3-ADP to S1 with an efficiency of 0.2 mol/mol ATPase site; the amount of incorporation was dependent on the duration of UV irradiation and saturated within 3 min. Analysis of S1 using SDS-PAGE following mild trypsinization revealed that Mant-8-N_3-ADP fluorescence was present only in the 20-kDa fragment (Fig. 2). By modeling of the 3D structure of skeletal muscle myosin using the 3D coordination data (pdb. 2MYS), we determined that Mant-8-N_3-ADP must be crosslinked to loop M, since the 20-kDa fragment intersects the ATPase site only in the region of loop M (677-689) (Fig. 1A). In particular, the methylated side chain of Lys 681 protrudes into the ATP-binding cleft and is situated such that it is highly likely to be crosslinked to Mant-8-N_3-ADP trapped within the ATPase site (Fig. 1B).

TABLE I. **Efficiencies of trapping and photolabeling of Mant-8-N_3-ADP by BeFn.**

Sample	Trapped Mant-8-N_3-ADP (mol/mol site)	Photoincorporated Mant-8-N_3-ADP (mol/mol site)
1	0.74	0.22
2	0.75	0.24
3	0.76	0.25

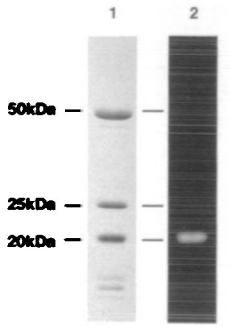

Fig. 2. **Localization of Mant-8-N_3-ADP labeling of S1 by limited tryptic digestion and SDS-PAGE.** The S1/Mg^{2+}-Mant-8-N_3-ADP/BeFn complex was prepared and irradiated as described under "MATERIALS AND METHODS," then digested with 1:100 (w/w) trypsin for 30 min. The tryptic fragments were separated on 7.5-20% acrylamide gradient slab gel. Lane 1, protein staining with Coomassie Brilliant Blue; lane 2, fluorescence of Mant-group crosslinked to the tryptic fragment under UV illumination at 366 nm.

Enzymatic Activity of Purified S1 Labeled with Mant-8-N_3-ADP (Mant-S1)—Divalent cation dependent ATPase activity of purified Mant-S1 (22% labeled) was measured and shown in Table II. EDTA(K^+)-ATPase activity was significantly reduced to 15%, and Ca^{2+}-ATPase was reduced to 60% by Mant-8-N_3-ADP labeling of S1. In contrast, the Mg^{2+}-ATPase activity of Mant-S1 was about 8-9 times greater than that of unlabeled S1. Moreover, upon activation with actin, the rate of Mg^{2+}-ATP hydrolysis by Mant-S1 was approximately two times higher than that by unlabeled S1 (Table II). These data show that Mant-S1 hydrolyzes ATP in the presence of Mg^{2+} at a greater rate than unlabeled S1, even when loop M has been covalently photolabeled with an ADP analogue, suggesting that the ATPase site is not blocked by the ADP analogue. This is consistent with the observation by Luo *et al.* (*11*) that the S1s labeled at loop B (320-327) and loop N (127-136) with Bz_2-εADP and NANDP respectively trapped by Vi have normal Mg^{2+}-ATPase activities. These results suggest the ADP analogues crosslinked into the loops at the edge of ATP-binding cleft are able to swing out of the active site by Mg^{2+}-ATP binding.

Fluorescence Polarization of Mant-S1—The polarization

TABLE II. **ATPase activities of S1 photolabeled with Mant-8-N_3-ADP.**

	(P_i mol/S1 mol/min at 25°C) S1	Mant-S1[b]
Mg^{2+}-ATPase	0.6	1.7
Mg^{2+}-ATPase (+actin)[a]	30.6	64.4
Ca^{2+}-ATPase	62.0	56.5
EDTA(K^+)-ATPase	150.2	122.1

[a]2 mg/ml = 46.5 μM. [b]Mant-S1 22.0% labeled.

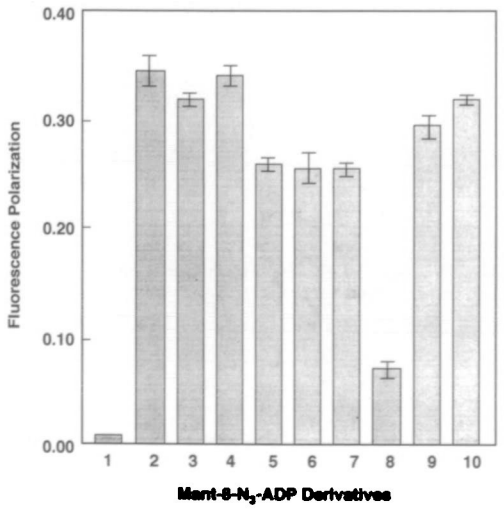

Fig. 3. **Polarization of the fluorescent emissions of Mant-8-N_3-ADP derivatives.** (1) Free Mant-8-N_3-ADP; (2) S1/Mant-8-N_3-ADP/BeFn complex; (3) Mant-S1; (4) Mant-S1 + 1 mM BeFn; (5) Mant-S1 + 2 mM ATP; (6) Mant-S1 + 2.5 μM actin; (7) Mant-S1 + 2 mM Mg^{2+}-ATP and 2.5 μM actin; (8) Mant-S1 + 5 M guanidine-HCl; (9) Mant-S1 + 2 mM EDTA and ATP; (10) Mant-S1 + 2 mM Ca^{2+} and ATP. Samples (1)-(8) were measured in the buffer of 120 mM NaCl and 30 mM Tris-HCl (pH 7.5), sample (9) in 0.5 M KCl. The excitation and emission wavelengths were 360 and 445 nm. The error bars represent the standard deviation from the mean of three to five experiments.

of Mant-group fluorescence was measured in order to observe the effects of Mg^{2+}-ATP and actin on the mobility of Mant-8-N_3-ADP cross-linked to loop M (677-689) (Fig. 3). The polarization of Mant-8-N_3-ADP increased dramatically when it was trapped within the ATP-binding cleft (Fig. 3; bars 1 and 2). This increase in polarization reflects the large reduction in rotational mobility of the probe resulting from the formation of a stable S1/Mg^{2+}-Mant-8-N_3-ADP/BeFn ternary complex. Mant-S1 also exhibited a high degree of fluorescence polarization, which was only slightly less than that seen when Mant-8-N_3-ADP was noncovalently trapped within the ATPase site (Fig. 3, bar 3). Addition of 1 mM BeFn increased polarization of Mant-S1 to the same level as the S1/Mg^{2+}-Mant-8-N_3-ADP/BeFn ternary complex (Fig. 3, bar 4). A significant increase in probe mobility, reflected by a decrease in Mant-S1 fluorescence polarization, was elicited by addition of Mg^{2+}-ATP (Fig. 3, bar 5). The increased probe mobility is consistent with Mg^{2+}-ATP competitively displacing Mant-8-N_3-ADP from the ATP-binding site to a less hindered site outside of the ATP-binding cleft. Interestingly, addition of actin, which does not bind to the ATPase site (Fig. 1A), induced a similar increase in probe mobility (Fig. 3, bar 6). Moreover, in the presence of actin, Mg^{2+}-ATP produced no additional changes in probe mobility (Fig. 3, bar 7). Considered together, these observations suggest that actin binding induces a conformational change at loop M (677-689) which results in dissociation of Mant-8-N_3-ADP from the ATP-binding site. Therefore, in the presence of actin, Mg^{2+}-ATP fails to increase probe mobility because, under the circumstances, it can no longer displace Mant-8-N_3-ADP. EDTA(K^+)-ATP and Ca^{2+}-ATP had little effect on Mant fluorescence polarization (Fig. 3, bars 9 and 10), which is consistent with their lower affinity for the ATP-binding site and their failure to increase Mant-S1 ATPase activity (Table II). As a control, fluorescence polarization of highly mobile free Mant-8-N_3-ADP and guanidine-HCl-denatured Mant-S1 were measured. They showed very low polarization (bars 1 and 8), confirming that the polarization measurements reflected the mobility of the Mant-group. As shown in Fig. 4, the slope of the Perrin plot in the presence of actin was not significantly different from that of control, suggesting that the binding of actin does not induce major global conformational change in Mant-S1. However, in the presence of ATP, the slope of the plot increased very slightly, which may reflect a global conformational change of Mant-S1 due to formation of the rounded or bent shape reported by Wakabayashi *et al.* on the basis of small angle X-ray scattering (*26*). In contrast, the extrapolated value of $1/P_0'$ estimated from the plot in the presence of ATP or actin significantly different from that of control. This result suggested that the localized mobility of Mant-group was increased by binding of ATP or actin to Mant-S1. The ATP binding may directly displace and swing out the Mant-8-N_3-ADP from the ATPase site, and the actin binding may allosterically swing the probe outside from the ATPase site due to conformational change of the loop M (677-689), resulting in increase mobility of the Mant-group.

Acrylamide Quenching of Mant-S1 Fluorescence—If Mant-8-N_3-ADP is displaced from the ATP-binding cleft by Mg^{2+}-ATP and/or actin, the fluorescent Mant-group should then be more accessible to the ambient solution and to dissolved quenching compounds such as acrylamide. To test this, Mant-S1 fluorescence was measured under conditions identical to those described in Fig. 3 (F_0) as well as with the addition of 20-100 mM acrylamide (F). Stern-Volmer quench curves (*14, 15*) were then constructed (Fig. 5) and the quench constants (K_{sv}) calculated. In the absence of ATP and actin, the quench constant for Mant-S1 was calculated to be 1.07 M^{-1} (Fig. 5, open circles), while that of Mant-8-N_3-ADP free in solution was 3.9 M^{-1} (Fig. 5, filled circles). In the former case, the lower quench constant

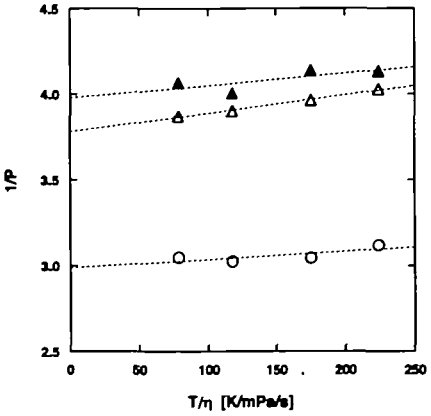

Fig. 4. **Perrin plots of the fluorescence polarization of Mant-S1 in the presence of actin or ATP.** Samples were measured in the buffer of 120 mM NaCl and 30 mM Tris-HCl (pH 7.5) containing 5, 10, 20, or 30% glycerol (○) in the presence of 2 mM ATP (△) or 2.5 μM actin (▲) at 15°C. The excitation and emission wavelengths were 360 and 445 nm.

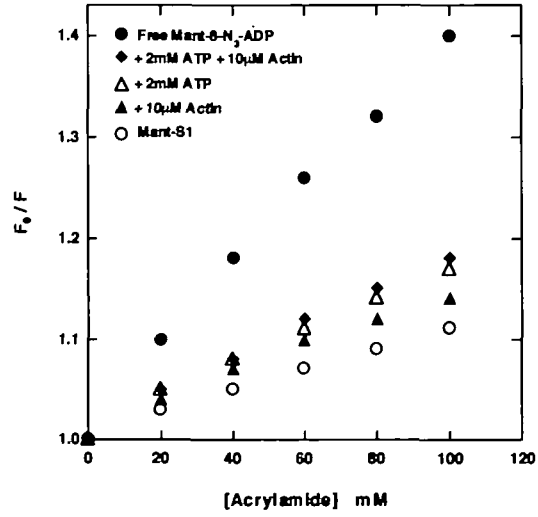

Fig. 5. **Stern-Volmer plots characterizing acrylamide quenching of the fluorescence of Mant-8-N_3-ADP derivatives.** 1 μM free Mant-8-N_3-ADP (●), 0.5 μM Mant-S1 (○), 0.5 μM Mant-S1+10 μM Actin (▲), 0.5 μM Mant-S1+2 mM ATP (△), 0.5 μM Mant-S1+2 mM ATP+10 μM Actin (◆). The assay was performed in the buffer of 30 mM Tris-HCl (pH 7.5) containing 120 mM NaCl and 2 mM $MgCl_2$ at 25°C. The excitation and emission wavelengths were 360 and 445 nm, respectively. Mant-S1 was prepared as described in "MATERIALS AND METHODS," and the amount of photoincorporated Mant-S1 was estimated to be 22.5% from the fluorescence intensity in 5 M guanidine-HCl, 20 mM Tris-HCl (pH 7.5).

illustrates that Mant-8-N_3-ADP was relatively inaccessible to dissolved acrylamide when bound inside the ATP binding cleft. Addition of either ATP (Fig. 5, open triangles) or actin (Fig. 5, filled triangles) increased exposure of Mant-8-N_3-ADP to the solvent, as indicated by increases in K_{sv} to 1.64 and 1.37 M^{-1}, respectively, which is consistent with the increased rotational mobility of the probe (Fig. 3). And consistent with their effect on fluorescence polarization, ATP- and actin-induced changes in K_{sv} were not additive (filled diamond; $K_{sv} = 1.65\ M^{-1}$). These findings suggest that the binding of either ATP or actin results in translocation of Mant-8-N_3-ADP from the ATP-binding cleft to a site outside the cleft which is less hindered and more accessible to the surrounding solution.

DISCUSSION

Recent crystallographic studies of the motor proteins, skeletal muscle myosin and kinesin, revealed that their motor domains have very similar structures (*4, 5, 18*). In addition, the amino acid sequences of the P-loop, Switch I, and Switch II were also highly conserved, suggesting that the two ATPases may generate energy for motility from ATP hydrolysis by the same molecular mechanism. Nevertheless, myosin possesses 3 unique loops [loop M (677-689), loop N (127-136), and loop B (320-327)] containing Lys 681, Trp 130, and Ser 324, respectively, which appear to be strategically situated around and within the ATP-binding cleft (Fig. 1). These loops, therefore, may be critical for determining the characteristic properties of myosin: *e.g.*, they may link the ATP-binding site to other regulatory regions of the myosin molecule.

Covalent labeling of loops B (320-327), N (127-136), and now M (677-689) with fluorescent ATP analogues has proved to be a useful method for studying loop function. NANDP has been incorporated into loop N (127-136) at the 130 Trp (*16*), and Loop B (320-327) has been labeled with Bz_2ADP at the Ser 324 (*17*). The precise functions of loops N (127-136) and B (320-327) remain unclear; but Luo *et al.* (*11*) found that actin binding has minimal effects on those loops. We previously showed that, when S1 was UV irradiated in the presence of excess molar Mant-8-N_3-ATP, the ATP analogue was covalently crosslinked to the 20-kDa fragment in the region of Lys 681 (*6*). In this study, we present evidence that a conformational change in loop M (677-689), a segment of the 20-kDa fragment containing Lys 681, is important in mediating actin-induced dissociation of reaction products from the ATP-binding cleft. To accomplish this, loop M (677-689) was photoaffinity labeled with the fluorescent ADP analogue, Mant-8-N_3-ADP, which was then used to monitor conformational changes in the loop.

Several pieces of evidence suggest that Lys 681 was site of Mant-8-N_3-ADP linkage to loop M (677-689). First, Mant-8-N_3-ADP is sufficiently long and the side chain of Lys 681 protrudes sufficiently into the ATP-binding cleft for Lys 681 to react with the entrapped Mant-8-N_3-ADP. Second, the crystal structure of *Dictyostelium* S1 revealed that the adenine ring of ATP is folded over near Arg 131 (identical to Trp 130 of Skeletal S1; *4*). However, because of the restricted conformation at the *N*-glycoside bond, the 8-azido moiety of Mant-8-N_3-ADP probably faces toward the side chain of Lys 681. This unusual binding conformation of Mant-8-N_3-ADP within the ATP-binding cleft may explain why Mg^{2+}-Mant-8-N_3-ATP and other bulky 8-substituted ATP analogues are hydrolyzed at a greater rate than ATP itself (*6, 19*). Finally, complete digestion of the Mant-8-N_3-ADP-labeled 20-kDa fragment by lysyl-endopeptidase yielded the peptide Leu 660-Lys 702, containing Lys 681 (*6*). It might be expected that modification of Lys 681 by Mant-8-N_3-ADP would prevent the hydrolysis at Lys 681 which otherwise would have occurred. Moreover, Chen *et al.* demonstrated that a photoaffinity labeling ATP analogue which carries a bulky spin probe at a position identical to ribose of regular ATP, crosslinked to the 20-kDa fragment by UV irradiation, suggesting that Lys 681 is a crosslinkable residue (*25*). Labeling loop M (677-689) with Mant-8-N_3-ADP did not antagonize hydrolysis of Mg^{2+}-ATP or actin binding (Table II). The rate of Mg^{2+}-ATP hydrolysis by Mant-S1 was within the normal range, suggesting that when covalently linked to the ATP-binding cleft, Mant-8-N_3-ADP was able to swing out of the active site and permit Mg^{2+}-ATP to bind and be hydrolyzed. Similarly, actin augmented Mg^{2+}-ATP hydrolysis by Mant-S1 to approximately the same degree as was seen with unmodified S1 (Table II); thus, actin binding was also unaffected by Mant-8-N_3-ADP labeling. In analogous fashion, specific modification of Trp 130 with a 2-hydroxy-5-nitrobenzyl group also had no affect on actin-facilitated Mg^{2+}-ATPase activity (*20*). It appears, therefore, that conformational changes in loop M (677-689), which is associated with myosin function, can be usefully monitored with a covalently linked fluorescent probe.

Mant-S1 fluorescence was highly polarized, but slightly less so than that of the S1/Mant-8-N_3-ADP/BeFn ternary complex. Addition of Mg^{2+}-ATP significantly decreased polarization of Mant-S1, while increasing K_{sv} (Figs. 3 and 5). Thus, ATP, which should competitively antagonize Mant-8-N_3-ADP binding within the ATP-binding cleft, displaced Mant-8-N_3-ADP to a site that was more accessible to the solvent and where rotational mobility of the fluorescent Mant-group was increased. Actin similarly decreased polarization of Mant-8-N_3-ADP and increased K_{sv} (Figs. 3 and 5), but actin does not bind directly to the ATP-binding cleft (Fig. 1A). Therefore, antagonism of Mant-8-N_3-ADP binding by actin must have been non-competitive in nature, and a conformational change in loop M seems a likely mechanism. Ca^{2+}- and EDTA(K^+)-ATP had negligible effects on polarization, consistent with the findings of lower activities of Ca^{2+}- and EDTA(K^+)-ATP hydrolysis (Table II) and the weaker binding of ATP to myosin in the absence of Mg^{2+} (*21*).

The data presented suggest that the surface loop M (677-689) at the end of the ATPase-site cleft, which is part of the 20-kDa fragment, may work as a signal transducer communicating between the actin-binding site and the ATP-binding site along the 20-kDa fragment. Previous studies demonstrating that modification of SH1 and SH2 affected both ATPase activity and actin binding support this idea (*22, 23*). Moreover, Ho and Chisholm (*24*) recently showed that mutations in the *Dictyostelium* myosin essential light chain bound to the helix tail of myosin head, lead to reduced actin-activated ATPase activity despite stoichiometric binding to the helix of the heavy chain. This may also suggest signal transduction along the backbone helix of the 20-kDa fragment *via* loop M (677-689). We anticipate that

further study of the 20-kDa fragment, including loop M (677-689), will provide additional new information on the complex sequence of enzymatic and mechanical events characteristic of myosin function.

We thank Dr. Toshiaki Arata (Osaka University) for helpful discussion.

REFERENCES

1. Cooke, R. (1986) The mechanism of muscle contraction. *CRC Crit. Rev. Biochem.* **21**, 53-118
2. Eisenberg, E. and Green, L.E. (1980) The relation of muscle biochemistry to muscle physiology. *Annu. Rev. Physiol.* **42**, 293-309
3. Bagshaw, C.R. and Trentham, D.R. (1973) The reversibility of adenosine triphosphate cleavage by myosin. *Biochem. J.* **133**, 323-328
4. Fisher, A.J., Smith, C.A., Thoden, J.B., Smith, R., Sutoh, K., Holden, H.M., and Rayment, I. (1995) X-ray structures of the myosin motor domain of *Dictyostelium discoideum* complexed with MgADP·BeFx and MgADP·AlF_4^-. *Biochemistry* **34**, 8960-8972
5. Kull, F.J., Sablin, E.P., Lau, R., Fletterick, R.J., and Vale, R.D. (1996) Crystal structure of the kinesin motor domain reveals a structural similarity to myosin. *Nature* **380**, 550-555
6. Maruta, S., Miyanishi, T., and Matsuda, G. (1989) Localization of the ATP-binding site in the 23-kDa and 20-kDa regions of the heavy chain of the skeletal muscle myosin head. *Eur. J. Biochem.* **184**, 213-221
7. Perry, S.V. (1952) Myosin adenosinetriphosphatase. *Methods Enzymol.* **2**, 582-588
8. Weeds, A.G. and Taylor, R.S. (1975) Separation of subfragment-1 isoenzymes from rabbit skeletal muscle myosin. *Nature* **257**, 54-56
9. Pardee, J. and Spudich, J.A. (1982) Purification of muscle actin. *Methods Enzymol.* **85**, 164-182
10. Penefsky, H.S. (1977) Reversible binding of Pi by beef heart mitochondrial adenosine triphosphatase. *J. Biol. Chem.* **252**, 2891-2899
11. Luo, Y., Wang, D., Cremo, C.R., Pate, E., Cooke, R., and Yount, R.G. (1995) Photoaffinity ADP analogs as covalently attached reporter groups of the active site of myosin subfragment 1. *Biochemistry* **34**, 1978-1987
12. Laemmli, U.K. (1970) Cleavage of structural proteins during the assembly of the head of bacteriophage T4. *Nature* **227**, 680-685
13. Youngburg, G.E. and Youngburg, M.V. (1930) *J. Lab. Clin. Med.* **16**, 158-166
14. Lehrer, S.S. and Leavis, P.C. (1978) Solution quenching of protein fluorescence. *Methods Enzymol.* **49**, 222
15. Stern, O. and Volmer, M. (1919) Über die abklingungszeit der fluoreszenz. *Phys. Z.* **20**, 183
16. Okamoto, Y. and Yount, R.G. (1985) Identification of an active site peptide of skeletal myosin after photoaffinity labeling with *N*-(4-azido-2-nitrophenyl)-2-aminoethyl diphosphate. *Proc. Natl. Acad. Sci. USA* **82**, 1575-1579
17. Mahmood, R., Elzinga, M., and Yount, R.G. (1989) Serine-324 of myosin's heavy chain is photoaffinity-labeled by 3′(2′)-*O*-(4-benzoylbenzoyl) adenosine triphosphate. *Biochemistry* **28**, 3989-3995
18. Rayment, I., Rypniewski, W.R., Schmidt-Bäse, K., Smith, R., Tomchick, D., Benning, M.M., Winkelman, D.A., Wesenberg, G., and Holden, H.M. (1993) Three-dimensional structure of myosin subfragment-1: a molecular motor. *Science* **261**, 50-58
19. Takenaka, H., Ikehara, M., and Tonomura, Y. (1978) Interaction between actomyosin and 8-substituted ATP analogs. *Proc. Natl. Acad. Sci. USA* **75**, 4229-4233
20. Peyser, Y.M., Muhlrad, A., and Werber, M.M. (1990) Tryptophan-130 is the most reactive tryptophan residue in rabbit skeletal myosin subfragment-1. *FEBS Lett.* **259**, 346-348
21. Mandelkow, E.M. and Mandelkow, E. (1973) Fluorimetric studies on the influence of metal ions and chelators on the interaction between myosin and ATP. *FEBS Lett.* **33**, 161-166
22. Mulhern, S.A. and Eisenberg, E. (1978) Interaction of spin-labeled and *N*-(iodacetylaminoethyl)-5-naphthylamine-1-sulfonic acid SH1-blocked heavy meromyosin and myosin with actin and adenosine triphosphate. *Biochemistry* **17**, 4419-4425
23. Reisler, E. (1982) Sulfhydryl modification and labeling of myosin. *Methods Enzymol.* **85**, 84-93
24. Ho, G. and Chisholm, R.L. (1997) Substitution mutations in the myosin essential light chain lead to reduced actin-activated ATPase activity despite stoichiometric binding to the heavy chain. *J. Biol. Chem.* **272**, 4522-4527
25. Chen, X., Pate, E., Cook, R., and Yount, R. (1998) A novel restricted photoaffinity non-nucleotide spin-labeled ATP analog: synthesis, characterization and interaction with myosin and muscle fibers. *Biophys. J.* **74**, A267
26. Wakabayashi, K., Tokunaga, M., Kohno, I., Sugimoto, Y., Hamanaka, T., Takezawa, Y., Wakabayashi, T., and Amemiya, Y. (1992) Small-angle synchrotron x-ray scattering reveals distinct shape changes of the myosin head during hydrolysis of ATP. *Science* **258**, 443-447